ORIGINAL ARTICLE

Spatiotemporal control of estrogen-responsive transcription in ERα-positive breast cancer cells

P-Y Hsu[1], H-K Hsu[1], T-H Hsiao[2,3,4], Z Ye[1], E Wang[5], AL Profit[3,6], I Jatoi[3,7], Y Chen[2,3,8], NB Kirma[1], VX Jin[1,8], ZD Sharp[1,3] and TH-M Huang[1,3]

Recruitment of transcription machinery to target promoters for aberrant gene expression has been well studied, but underlying control directed by distant-acting enhancers remains unclear in cancer development. Our previous study demonstrated that distant estrogen response elements (DEREs) located on chromosome 20q13 are frequently amplified and translocated to other chromosomes in ERα-positive breast cancer cells. In this study, we used three-dimensional interphase fluorescence in situ hybridization to decipher spatiotemporal gathering of multiple DEREs in the nucleus. Upon estrogen stimulation, scattered 20q13 DEREs were mobilized to form regulatory depots for synchronized gene expression of target loci. A chromosome conformation capture assay coupled with chromatin immunoprecipitation further uncovered that ERα-bound regulatory depots are tethered to heterochromatin protein 1 (HP1) for coordinated chromatin movement and histone modifications of target loci, resulting in transcription repression. Neutralizing HP1 function dysregulated the formation of DERE-involved regulatory depots and transcription inactivation of candidate tumor-suppressor genes. Deletion of amplified DEREs using the CRISPR/Cas9 genomic-editing system profoundly altered transcriptional profiles of proliferation-associated signaling networks, resulting in reduction of cancer cell growth. These findings reveal a formerly uncharacterized feature wherein multiple copies of the amplicon congregate as transcriptional units in the nucleus for synchronous regulation of function-related loci in tumorigenesis. Disruption of their assembly can be a new strategy for treating breast cancers and other malignancies.

Oncogene (2016) 35, 2379–2389; doi:10.1038/onc.2015.298; published online 24 August 2015

INTRODUCTION

Activated estrogen signaling is known to induce nuclear translocation of estrogen receptor alpha (ERα) to bind estrogen-responsive elements nearby target promoters for gene transcription.[1–3] This hormone-driven genomic action of ERα is proved to have a vital role in promoting aberrant proliferation of luminal breast cancers.[1–5] Recent studies additionally demonstrated that estrogen stimulation triggers ERα binding to distant estrogen response elements (DEREs), which are located far away from target loci on the same or different chromosomes, to cause intra- or inter-chromatin interactions that bring the ERα–DERE complex to target promoters for transcriptional modulation.[5–7] However, this traditional view of one-to-one interaction between an enhancer and an individual promoter has recently been challenged by emerging observations that multiple estrogen-responsive loci may be choreographically regulated in a spatio-temporal manner.[6,7]

Increased evidence reveals that transcription units are frequently clustered in a discrete focal site within the nucleus, termed regulatory depot or transcription factory.[8–11] Instead of recruiting and assembling each transcription unit to a target locus, genes localized on different chromosomes are brought to a preassembled regulatory depot for transcriptional action.[8–10] Early work showed that genes of the same family are prone to

congregate to particular substructures of the nucleus, including promyelocytic leukemia bodies for the major histocompatibility locus and Cajal bodies for histone loci.[11–13] Subsequent studies reported that genes respectively encoding interleukins and cytokines are frequently clustered together in the nucleus, presumably analogous to specialized regulatory units for concurrent transcription.[11,14,15]

In gene silencing, a regulatory depot may drive enhancer–promoter crosstalk through cooperative interactions between chromatin insulators and polycomb complexes.[16–19] Moreover, epigenetic changes, including post-translational modifications on histone H3 lysine residues, addition of methyl group on DNA cytosine bases and occupancy switch of chromatin remodeling proteins, contribute to this transcription repression.[17–19] Histone modifications, such as H3K27me3 and/or H3K9me3, are also frequently found in methylated promoter regions.[17] These modifications alter chromatin configuration through limiting the accessibility of transcriptional units to RNA polymerase II and associated co-factors.[10,17–19]

Our recent studies indicated that prolonged estrogen exposure triggers dynamic chromatin interactions for DERE-mediated transcription repression implicated in breast tumorigenesis.[5,7] Extensive genome mapping identified clustered DEREs originally located on 20q13 that were frequently inserted into multiple

[1]Department of Molecular Medicine, Institute of Biotechnology, The University of Texas Health Science Center at San Antonio, San Antonio, TX, USA; [2]Greehey Children's Cancer Research Institute, The University of Texas Health Science Center at San Antonio, San Antonio, TX, USA; [3]Cancer Therapy and Research Center, The University of Texas Health Science Center at San Antonio, San Antonio, TX, USA; [4]Department of Medical Research, Taichung Veterans General Hospital, Taichung City, Taiwan; [5]Department of Cellular and Structural Biology, The University of Texas Health Science Center at San Antonio, San Antonio, TX, USA; [6]Department of Pathology, The University of Texas Health Science Center at San Antonio, San Antonio, TX, USA; [7]Department of Surgery, The University of Texas Health Science Center at San Antonio, San Antonio TX, USA and [8]Department of Epidemiology and Biostatistics, The University of Texas Health Science Center at San Antonio, San Antonio, TX, USA. Correspondence: Dr TH-M Huang, Department of Molecular Medicine, Institute of Biotechnology, The University of Texas Health Science Center at San Antonio, STRF 300.31, 8403 Floyd Curl Drive, San Antonio, TX 78229, USA.
E-mail: huangt3@uthscsa.edu
Received 30 January 2015; revised 20 June 2015; accepted 5 July 2015; published online 24 August 2015

genomic sites, resulting in complex chromosomal rearrangements and amplification, analogous to the phenomenon of chromothripsis.[7,20] Although 20q13 DEREs were found to scatter in multiple sites,[7] in this study, we first sought to determine if these amplicons may be clustered together in the nucleus as a regulatory unit for simultaneous transcription control. We also investigated if heterochromatin protein1 (HP1) participates in coordinating DERE-directed chromatin movement and transcriptional regulation. By pharmacologically and genetically disrupting the DERE target assembly, we also assessed functional consequences of these amplicons in the development of luminal breast cancers.

RESULTS

Repressive epigenetic machinery preferentially occupies neighboring regions of DEREs on 20q13

Integration of our published chromosome conformation capture (3C)-seq and ER ChIP-seq data sets,[7] chromosome 20q13 harboring dense DERE sites was found to have a high frequency of estrogen-driven chromatin interactions in the genome (see the circos plot in Figure 1a). To understand DERE-involved transcription control through chromatin looping, we surveyed the occupancy of histone marks and DNA methylation patterns in a 10-Mb region of 20q13.[7,21] Repressive epigenetic modifications, including H3K9me3, H3K27me3 and DNA methylation, dominated the neighboring regions of the examined DERE sites with amplification (see a highlighted area in Figure 1a). Correlation analysis of the examined ERα-bounded DERE sites with these epigenetic marks additionally indicated that amplified DEREs were prone to suppress gene expression through interactions with these neighboring regions (Figures 1b–e). chromatin immunoprecipitation (ChIP)-quantitative PCR (qPCR) analyses of histone

alterations provided supportive evidence that repressive marks —H3K27me3 and H3K9me3 are relatively enriched in nearby DEREs compared with active marks—H3K4me3, H3K9ac and H3K27ac (Supplementary Figure 1).

To further interrogate the involvement of DNA modification in DERE-mediated transcription control, we mapped DNA methylation patterns of 20q13 DEREs and the associated flanking regions (−2.5 to +2.5 kb) in 9 ERα-positive breast cancer cell lines—LY2, MCF-7, BT474, HCC1419, HCC1428, MDA-MB-175, SUM52PE, HCC1500 and 600MPE using our published methylation data set.[7,22] Correlation analysis indicated that increased DERE copies (5–149 copies) were positively linked to elevated DNA methylation levels in these cell lines (Figure 2a). Extensive analysis of long-range chromatin interactions in MCF-7 cells additionally revealed that less frequent or fewer looping events occur in hypermethylated DEREs compared with hypomethylated DERE sites in E2-treated breast cancer cells (Figure 2b). Moreover, hypermethylated DEREs observed in ERα-positive breast tumors were associated with poor overall survival of patients ($n = 37$, $P = 0.0005$; Figure 2c). We thus speculated that amplified DEREs potentially cooperate with the epigenetic machinery for long-range regulation, leading to the intensification of repression on target genes involved in cancer development of breast.

HP1-involved DERE clustering and spatiotemporal control of target gene expression

To study whether scattered DEREs gather as regulatory depots in the nucleus for estrogen-responsive transcription control, we performed interphase three-dimensional fluorescence in situ hybridization (3D-FISH) in MCF-7 cells treated with E2 for a period of 24 h. Estrogen stimulation led to a time-dependent clustering of amplified DEREs in 0.5 to 1 h, but these large loci were regressed
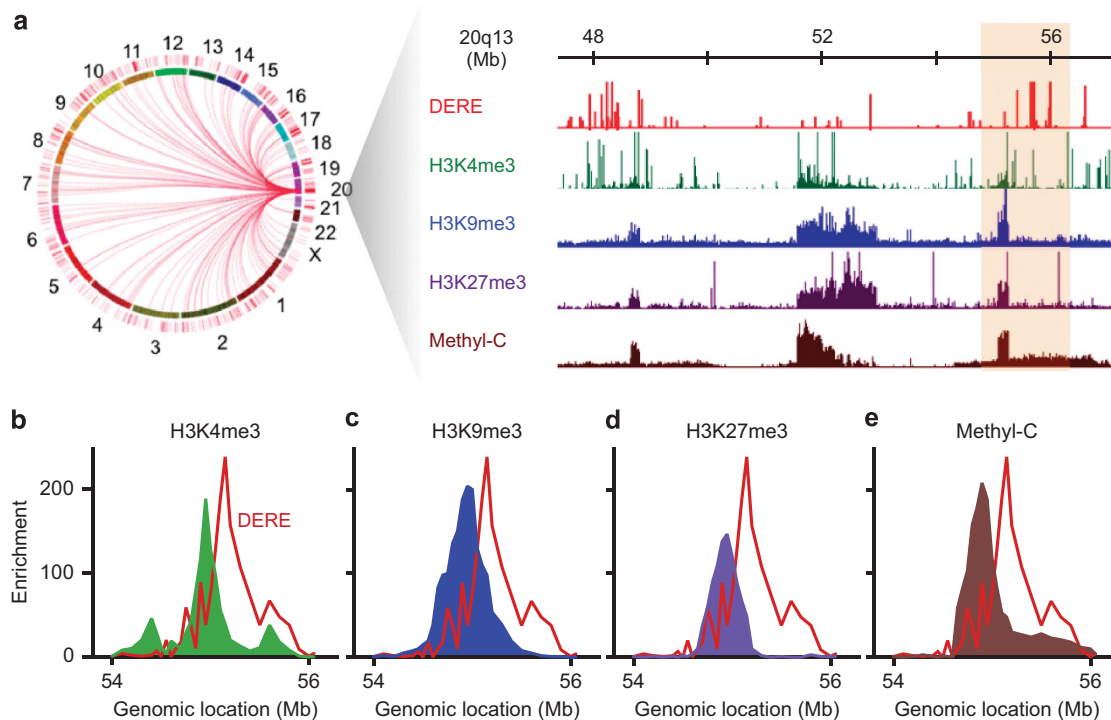

Figure 1. Repressive epigenetic marks occupy neighboring area of 20q13 DEREs. (**a**) Genomic landscapes illustrated the presence of epigenetic machinery and DERE sites in 20q13 region. A circos plot depicted 20q13 DERE-mediated chromatin interactions and DERE sites represented as red lines outside the chromosome circles. Three published data sets mapping DERE sites, estrogen-triggered RNA Pol II binding, occupancy of three histone marks and DNA methylation patterns (Methyl-C) were applied to plot the genomic landscapes.[7,21] High-lightened area: the amplified DERE region of interest. (**b–e**) Distribution of epigenetic marks was nearby the examined amplified DERE region. H3K4me3 in **b**; H3K9me3 in **c**; H3K27me3 in **d**; Methyl-C in **e**.
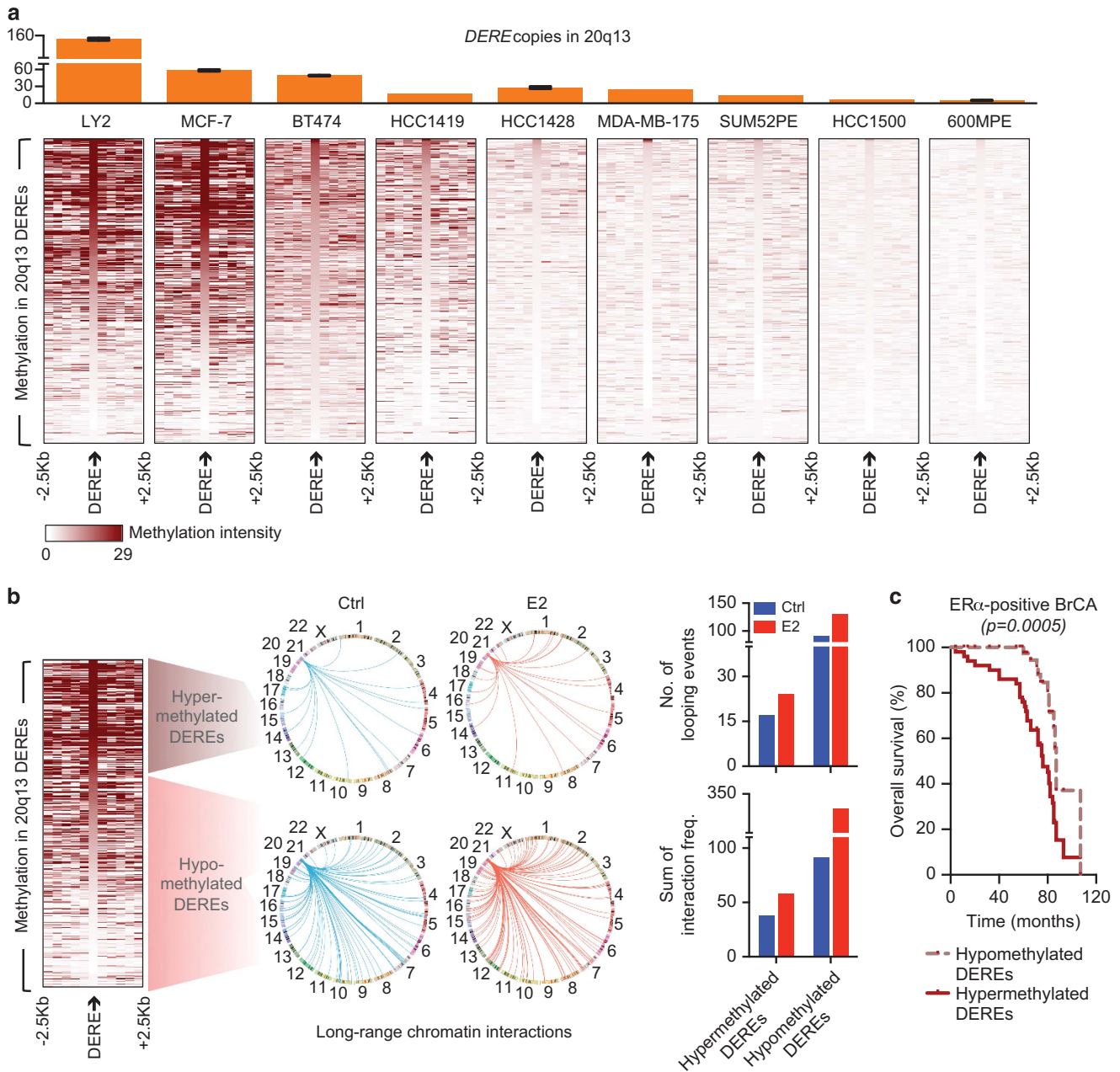
Figure 2. Positive correlation between DNA hypermethylation and DERE amplification links to adverse outcome. (**a**) Intensity maps of DNA methylation in ERα-positive breast cancer cells. A published MBDCap-seq data set for profiling DNA methylation was utilized to generate heat maps of methylation patterns in 20q13 DEREs (centered) and the flanking regions (−2.5 to +2.5 kb).[22] The histogram plot shows 20q13 DERE copies in each cell line.[7] (**b**) Inverse correlation between DNA methylation and DERE-directed long-range chromatin interactions. A heat map indicated DERE methylation patterns in MCF-7 cells as showed in (**a**). Circos plots described long-range chromatin interactions mapped by 3C-seq in hyper- and hypomethylated DERE regions at 20q13.[7] Histogram graphs were plotted to summarize the number of looping events and sum of interaction frequencies, respectively, in hyper- and hypomethylated DEREs upon estrogen stimulation. (**c**) Kaplan-Meier survival curves of 50 ERα-positive breast cancer patients harboring either hypo- (n = 13) or hypermethylated (n = 37) DEREs at 20q13. Mantel-Cox test was applied to determine statistical significance.

in 4 h (see inserted squares in Figure 3a). Accumulated DNA methylation was likely attributed to the immobilized DERE sites (Figure 2b).

As repressive histone marks were found to be enriched in the neighboring regions of DEREs and two-thirds (61 out of 92) of 20q13 DERE-targeted looping loci were suppressed by E2 (Figure 1 and Supplementary Figures 1 and 2), we hypothesized that the gatherings of these DEREs formed single regulatory units to synchronize gene repression. As HP1 is a well-known factor in silencing,[17,23] we used immuno-FISH to map its localization relative to DERE foci in MCF-7 cells stimulated with E2 (Figure 3b). Colocalization frequencies of *DERE*-HP1 were relatively higher at 0.5–1 h compared with other time points (see yellow signals in inserted squares and the histogram plot). ChIP-qPCR analysis of HP1 presenting on the examined *DERE* sites further confirmed *DERE*-HP1 colocalization on a higher genomic

resolution level (see 'Ctrl peptide' group in Supplementary Figure 3a). Importantly, estrogen-induced coupling was disrupted by a HP1 blocking peptide, which is known to targets an internal region harboring DNA-binding domain of HP1 (Figure 3c and 'HP1 blocking peptide' group in Supplementary Figure 3a).[24] In parallel, we also observed that 20q13 DEREs were no longer clustered in the nucleus as regulatory depots, profoundly altering the synchronized expression of ~80% (73 out of 92) target genes

(Figure 3d). These results suggest that HP1 may act as an anchor protein in regulating the assembly of DERE-mediated transcription assemblages.

DERE regulatory depot directs long-range epigenetic repression of an estrogen-responsive gene, *ZIM2*

To investigate the molecular events underlying DERE-mediated repression, we chose *ZIM2*, a potential tumor-suppressor gene
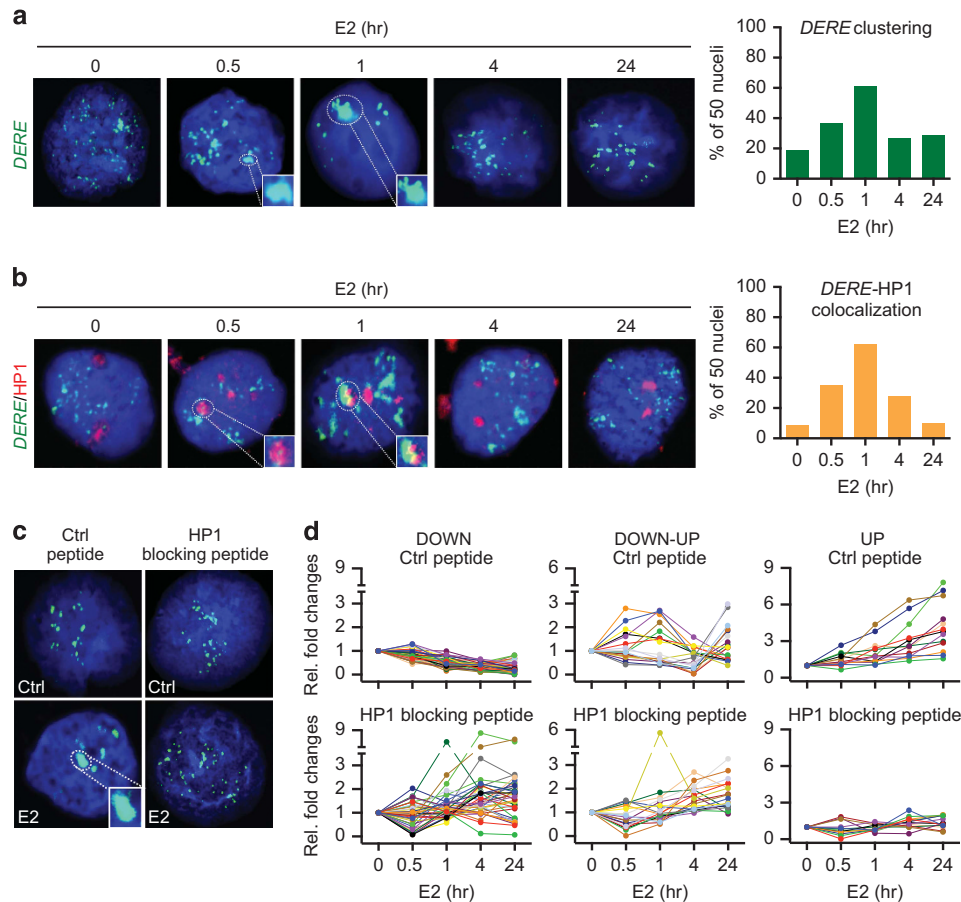

Figure 3. HP1 participates in estrogen-induced assembly of DERE-involved regulatory depots and associated transcriptional regulation. (**a** and **b**) Estrogen-triggered *DERE* clustering and *DERE*-HP1 colocalization. Hormone-deprived MCF-7 cells with E2 in different time periods as indicated were subjected to interphase 3D-FISH in (**a**) or immuno-FISH analysis in (**b**). A representative image per condition is showed. Inserted squares: clustered DEREs; *DERE*-HP1 colocalization. Quantifying frequency of *DERE* clustering and *DERE*-HP1 colocalization in 50 nuclei was summarized in histogram plots, respectively. (**c** and **d**) Blocking HP1 diminished estrogen-driven DERE clustering and transcription control of DERE-targeted loci. With pretreatment of control or HP1-blocking peptide, cells were stimulated with 1 h of dimethylsulfoxide (DMSO; Ctrl) or E2 for interphase 3D-FISH analysis in **c** or different time periods of E2 as indicated for RT–qPCR analysis in (**d**). Inserted square: clustered DEREs. Each line in the spike plots represents examined individual gene. The expression patterns of DERE-targeted genes as shown in **d** were categorized into three groups: constitutive downregulation (DOWN; left), down-then-upregulation (DOWN-UP; middle), and constitutive upregulation (UP; right).

Figure 4. Estrogen activates DERE-mediated long-range epigenetic transcription of a representative DERE-targeted gene, *ZIM2*. (**a**) Estrogen-induced *DERE-ZIM2* colocalization. Interphase 3D-FISH analysis was assayed on hormone-deprived MCF-7 cells treated with E2 in different time periods as indicated. A representative image per condition is showed. Inserted squares: *DERE-ZIM2* colocalization. Frequency counting of *DERE-ZIM2* colocalization in 50 nuclei was presented in a histogram graph. (**b**) Experimental scheme of a 3C-ChIP-qPCR approach. Looping assay (3C) was first conducted on cross-linked chromatin with *Bam*HI digestion and subsequent diluted ligation. DNA-IP assay (ChIP) was then performed to pull-down the protein binding on the looping events, following qPCR analysis of ligated fragments. (**c**) 3C-qPCR analyses of estrogen-induced *DERE-ZIM2* chromatin interactions. Upper panel: illustration of examined chromatin interactions between 20q13 DEREs and *ZIM2* locus. 20q13 DEREs were designated as 'baits' and three 'interrogated fragments' were showed in the promoter region of *ZIM2* locus after *Bam*HI digestion. Results are presented as relative interaction frequencies compared with those *GAPDH* as an internal control. (**d**) Occupancy analyses of participated proteins on estrogen-induced *DERE-ZIM2* looping. 3C-ChIP-qPCR analyses were performed to survey the presence of ERα, HP1, H3K4me3, H3K9me3, H3K27me3 and RNA Pol II. Mean ± s.d. (*n* = 6 replicates in two batches of treatment). *P < 0.05; **P < 0.01; ***P < 0.001 (Student's t-test), compared with control cells (time point '0 h'). All samples applied to either 3C- or 3C-ChIP-qPCR analysis were pretreated with a control peptide in before estrogen stimulation.

located on 19q13,[7,25] for detailed mechanistic studies. Similar to the dynamics of HP1-*DERE* coupling (Figure 3b), we found that estrogen stimulation triggered colocalization of one *ZIM2* allele with the clustered DEREs at 0.5 to 1 h (see yellow signals and the histogram plot in Figure 4a). This colocalization was linked to subsequent E2-driven repression of the gene (Figure 5a, green columns). It should be noted that the other copy of *ZIM2*, which is likely the maternally inactive allele,[25] was not mobilized to the DERE cluster.

3C-qPCR analysis confirmed preferential chromatin interactions between 20q13 DEREs and the *ZIM2* promoter at 0.5 h after E2 treatment (Figure 4c). We then used 3C-ChIP-qPCR, which combined both looping assay (3C) and ChIP-qPCR analysis in a sequential order, to dissect dynamic changes of epigenetic marks in the DERE-interacting *ZIM2* locus (see an example in Figure 4b). Our results showed that estrogen-induced *DERE–ZIM2* chromatin interactions with increasing binding of ERα to the region (Figures 4c and d). These interactions were accompanied with
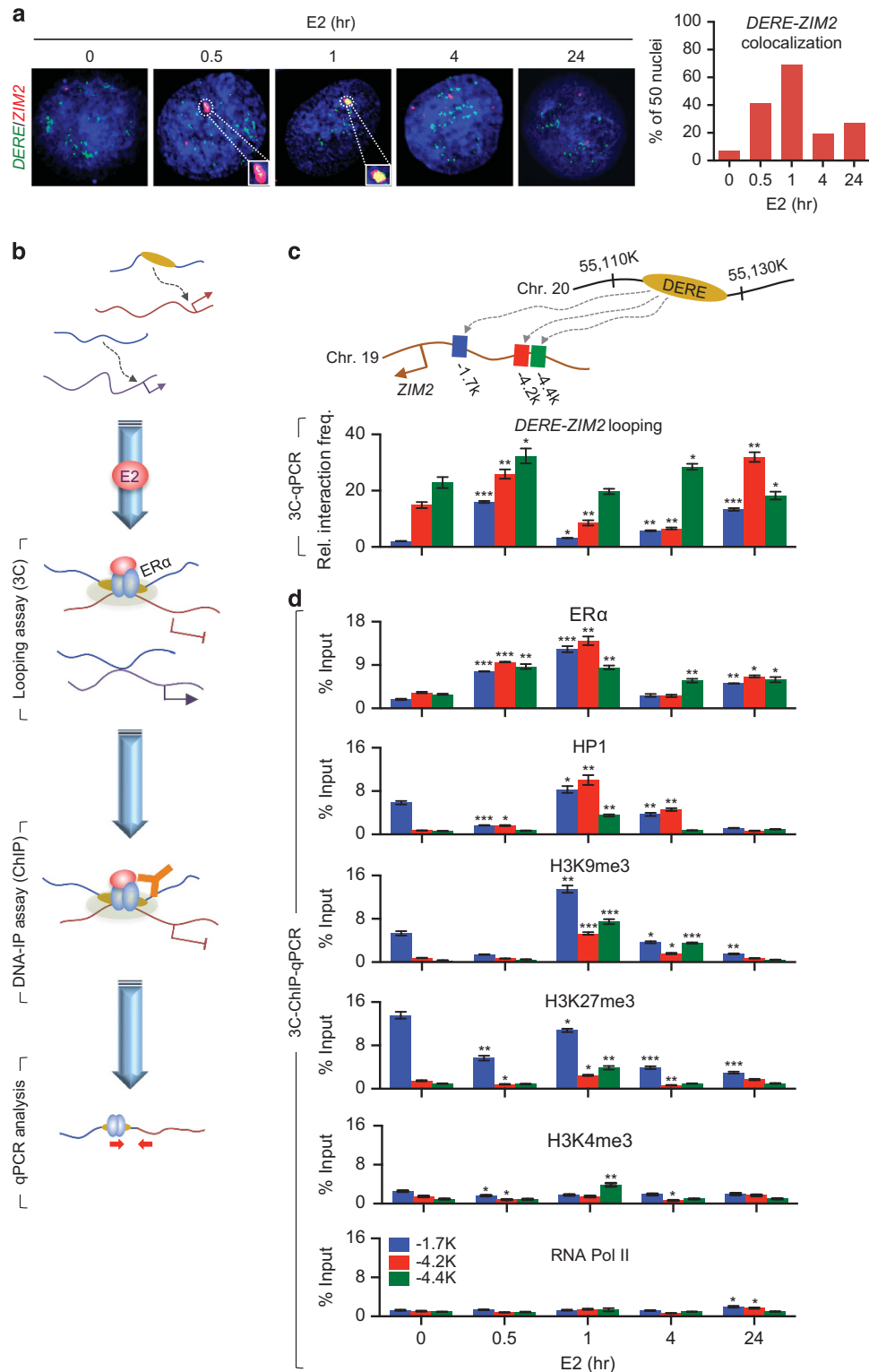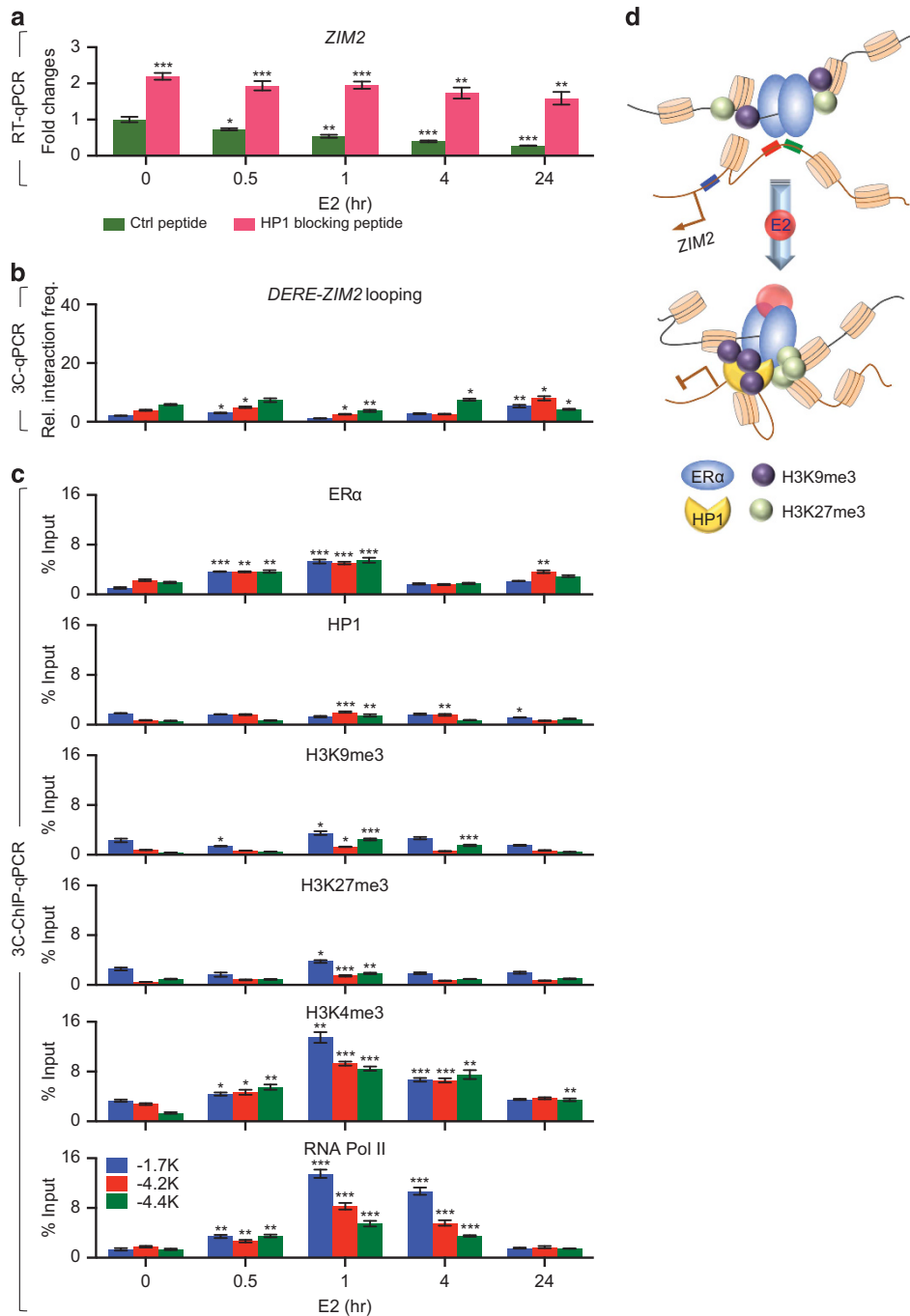
Figure 5. Neutralizing HP1 impairs DERE-involved long-range epigenetic repression of *ZIM2* upon estrogen stimulation. (**a–c**) Effect of HP1 blocking peptide on DERE-mediated long-range transcription of *ZIM2* upon estrogen stimulation. With pretreatment of a control peptide or HP1-blocking peptide in each time point, E2-treated cells as indicated were subjected to RT–qPCR analysis of *ZIM2* expression in **a**; 3C-qPCR analyses of *DERE-ZIM2* chromatin interactions in **b**; 3C-ChIP-qPCR analyses of associated proteins presenting on *DERE-ZIM2* looping in **c**. Mean ± s.d. (*n* = 6 replicates in two batches of treatment). *P < 0.05; **P < 0.01; ***P < 0.001 (Student's *t*-test), compared with control peptide-treated cells (time point '0 h'). (**d**) Proposed model of estrogen/DERE-driven long epigenetic repression of *ZIM2* with HP1 participation. Estrogen stimulation caused ERα binding on DEREs for inducing long-range *DERE-ZIM2* chromatin interactions, following recruitment of H3K27me3 and HP1-interacted H3K9me3 to *DERE-ZIM2* looping, leading to gene suppression.

increased levels of HP1 and repressive histone marks (H3K9me3 and H3K27me3) to *ZIM2* and in concert with low levels of the active mark H3K4me3 and RNA Pol II recruitment (Figures 4d, 1 h columns). In parallel, ChIP-qPCR analyses further demonstrated that estrogen treatment triggers the recruitment of ERα, HP1 and other repressive marks at *DERE*, not *ZIM2* (see 'Ctrl peptide' group in Supplementary Figures 4a and b). The E2-induced chromatin looping then brings

ZIM2 to this *DERE*-HP1 repressive complex for gene suppression. However, this epigenetically mediated gene silencing was significantly reversed by treatment with DNA methyltransferase inhibitor (5-aza-2'-deoxycytidine) and/or histone deacetylase inhibitor (trichostatin A) (Supplementary Figure 5).

The above findings indicated that HP1 may have a role in modulating DERE-directed epigenetic repression of *ZIM2*

(Figures 3b and d and 4d). With treatment of the HP1 blocking peptide, we found that both pre-formed and E2-induced DERE–ZIM2 chromatin interactions were impaired, resulting in the restoration of ZIM2 expression (Figures 5a and b). This treatment also prevented the appearance of HP1 and repressive histone marks, but not ERα, on DERE–ZIM2 chromatin loops and DERE sites. Instead, RNA Pol II and H3K4me3 were recruited to the ZIM2 locus confirmed the restoration of its expression (Figure 5c and 'HP1 blocking peptide' group in Supplementary Figures 4a and c). Furthermore, attenuation of HP1 expression using a specific small interfering RNA (siRNA) showed that ZIM2 expression was increased with less frequent looping and enhanced occupancy of active histone marks—H3K4me3 and RNA Pol II (Supplementary Figure 6). Treatment with this siRNA ($P = 0.005$) or the HP1 blocking peptide ($P < 0.0001$) additionally inhibited cell growth related to those scrambled siRNA-treated or control peptide-treated cells (Supplementary Figure 7). Taken together, these results illustrate that estrogen mobilizes one ZIM2 allele to an ERα–DERE regulatory depot via long-range chromatin movement. HP1 may act as a stabilizer in maintaining the pre-formed chromatin looping events for further repressive modifications (H3K9me3 and H3K27me3) of the ZIM2 locus, leading to gene silencing (Figure 5d).

CRISPR/Cas9-edited deletion of 20q13 DEREs attenuates Janus kinase (JAK)/signal transducer and activator of transcription (STAT) signaling networks for cancer cell proliferation with better overall survival

Our early study suggested that increased copy number of 20q13 DEREs correlated with reduced overall survival of ERα-positive breast cancer patients.[7] To genetically address the role of DEREs in estrogen-responsive gene expression and breast tumorigenesis, we used a single RNA-single protein genomic-editing system, CRISPR/Cas9,[26] to precisely delete a 1-kb region of 20q13 that harbors eight DERE sites in MCF-7 cells (Figure 6a). As shown in Figure 6b, PCR analysis of the targeted region (lanes 1 and 7) showed that two DERE/del constructs were generated, with partial deletion in #1 (lanes 2 and 8) and complete deletion in #2 (lanes 3 and 9). Time-lapse proliferation assays demonstrated the growth of DERE/del #2 cells was significantly prohibited relative to that of wild-type (Ctrl) cells ($P < 0.005$; Figure 6c). Expression analysis of this clone further uncovered that one-third (33 out of 92) of DERE-regulated loci were transcriptionally altered (Figure 6d and Supplementary Figure 8). For example, expression levels of apoptosis-related genes (for example, FOS), transcriptional repressors (for example, SIM2) and tumor suppressors (for example, IFIT2 and ZIM2) were increased,[7,27–30] but proliferation-related loci (for example, TRAP1 and TSPAN9) and tyrosine kinases/phosphates (for example, ERRB4, JAK1 and PTPRT) were repressed,[31–35] confirming the anti-proliferative phenotype of DERE/del #2 cells. Ingenuity pathway analysis of these 33 genes indicated that JAK/STAT signaling participated in DERE-modulated tumor growth and deletion of this DERE region may activate MYC/FOS-involved apoptotic signaling (Figure 6e).[27,28,36] An independent study of DERE/del clone #3 derived from another batch of DERE/del mutants confirmed that deletion of this 1-kb DERE region of interest profoundly reduces cell growth ($P = 0.0029$) and alters transcription profiles of DERE-targeted looping genes involved in JAK/STAT signaling (Supplementary Figure 9).

We additionally surveyed published expression data of two breast cancer cohorts to determine the clinical relevance of DERE-involved transcription regulation.[37,38] Kaplan–Meier analysis of 129 non-relapse tumors revealed that DERE/del-activated ($P < 0.0001$) or DERE/del-repressed ($P = 0.0087$) genes were significantly linked to longer overall survival of patients with ERα-positive breast cancer (Figure 6f).[37] A second cohort of 227 ERα-positive breast cancer patients implicated these DERE/del-regulated loci ($P < 0.0001$, activated; $P = 0.0028$, repressed) were correlated with long-lasting overall survival of patients without tumor recurrence after 5 years of tamoxifen therapy (Figure 6g).[38] This in silico analysis together with the in vitro findings support an important role of DERE regulatory depots in promoting advanced development of luminal breast cancer.

DISCUSSION

Amplification in chromosome 20q13 is frequently observed in breast tumors.[39–41] Although putative oncogenes, such as ZNF217 and MAP3K3, have been mapped to this region, their over-expression alone cannot sufficiently promote cancer development.[40,41] In this study, we demonstrated that amplified DEREs at 20q13 function as another potential oncogenic driver for luminal breast cancers. Estrogen stimulation triggered DERE copies ($n = 50–60$) congregated in 2–3 regulatory depots for synchronized transcription control of ~92 genes located on distinct chromosomes through long-range chromatin interactions, leading to activation of signaling cascades for aberrant proliferation of breast cancer cells. Importantly, 20q13 DEREs modulated the JAK/STAT signaling network that drives the proliferation of breast cancer cells (Figure 6). These findings provide promising evidence that the examined DEREs act is a proliferative driver for a subset of breast neoplasms. Instead of using one-enhancer–one-promoter chromatin interactions, cancer cells exploit this previously uncharacterized mechanism involving depots to regulate multi-gene expression through coordinated chromatin movement. This concurrent action greatly enhances aberrant cell proliferation. As this work only presents amplified 20q13 DEREs clustered as regulatory depots in breast cancer cells, other tumor models possibly have similar transcriptional modulation utilizing specific regulatory amplicons. Extensive studies will be needed to explore and characterize these regulatory depots and associated actions in concurrent transcription of multiple target genes for malignant progression.

The aforementioned concept of regulatory depots is in direct contrast to the general thinking that each transcription unit is preassembled with transcription factor(s) presenting on distant or proximal enhancer(s) and then mobilized to promoter regions of individual target locus through inter- or intra-chromatin interactions.[18,19] However, it cannot thoroughly explain the synchronized transcription alteration of multiple genes in cancer cells. Alternatively, the transcription factory model posits that target loci from different chromosomes are brought together to form a preassembled and immobilized regulatory center, which includes RNA Pol II modules and co-/regulators for concurrent transcription.[8–11] Our work shows an added layer of regulation by hormone stimulation that induces the formation of DERE regulatory depots with subsequent mobilization of estrogen-responsive genes to these centers through chromatin movement for transcriptional alteration. Moreover, it has been documented that spatial proximities are conductive to affect the incidence of chromosome translocations.[20,23,42] As a potential causation, our previous study found that estrogenic exposure enhances DERE-directed chromatin interactions, which potentially create fragile sites for genomic rearrangement and consequently lead to DERE amplification in breast tumorigenesis.[7] Using recruitment of the c-Myc locus to a Igh-related transcription factory as another example, frequent chromatin interactions may result in the prevalence of translocations with increased c-Myc copies in plasmacytomas and Burkitt's lymphoma.[23] These findings suggest that aberrant chromatin interactions coupled with repeat ampli-fication of regulatory elements spur tumor development by promoting transcriptional alteration of multiple oncogenes and tumor-suppressor genes to activate survival-related signaling network for tumorigenesis. Consequently, disassembling specific
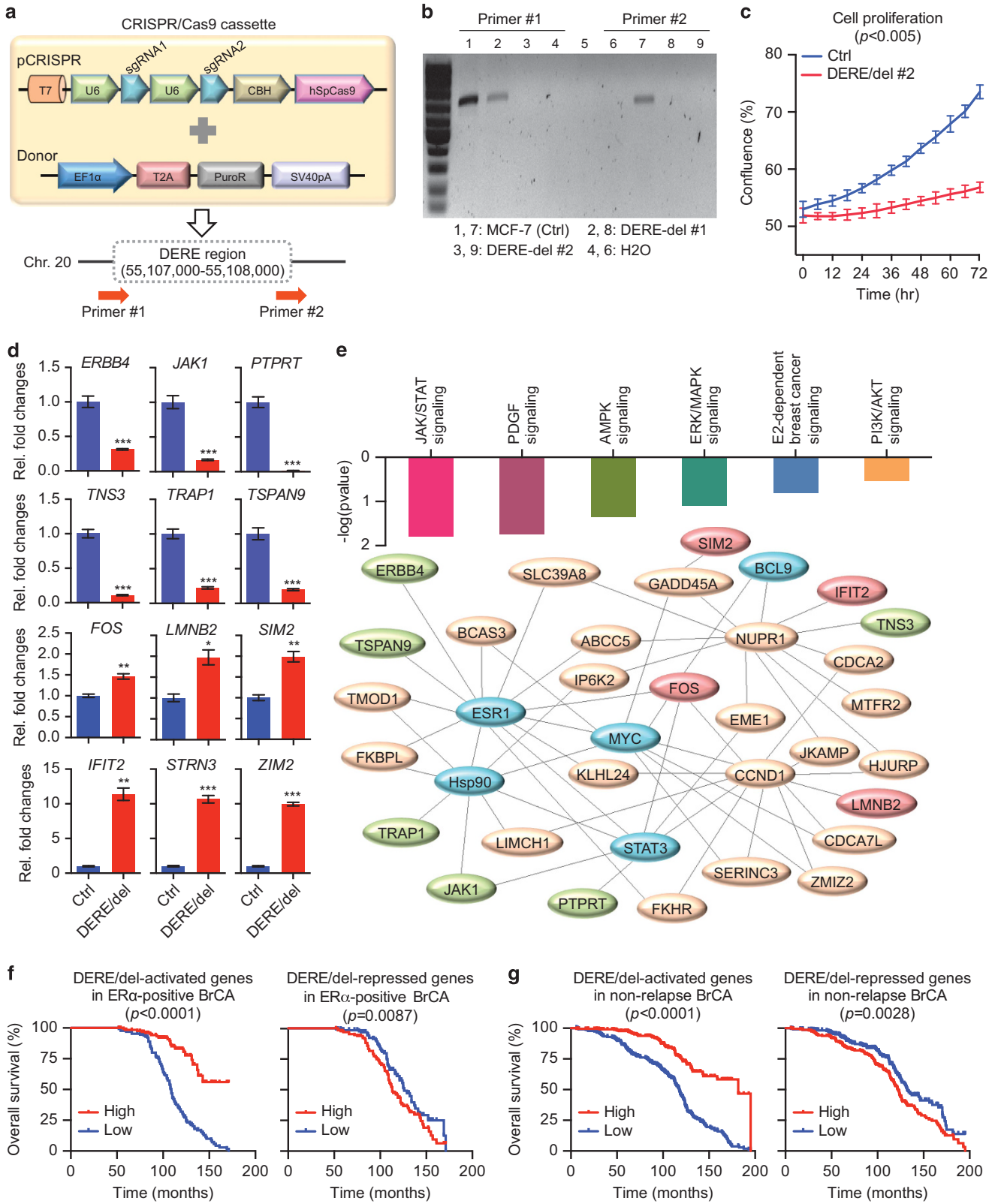
regulatory depots may be an efficient and comprehensive strategy of cancer therapy.

As a key factor and potential target for depot disassembly, we also found that the DERE regulatory depots tethered HP1 for coordinated chromatin movement and subsequent gene regulation in a spatiotemporal manner. HP1 is a fundamental unit of heterochromatin and acts as a transcriptional repressor through interacting with methylated H3K9 residues of histones, DNA methyltransferase and methyl CpG-binding proteins.[23,43,44] Using a DERE-targeted locus—ZIM2 as a test case (Figures 4 and 5 and Supplementary Figures 4 and 6), we additionally revealed that HP1 serves as a critical regulator in the DERE-directed long-range epigenetic gene repression. Specifically, neutralizing HP1 function with a blocking peptide defined a new role of this protein as a potential anchor protein for modulating the assembly of DERE regulatory depots (Figure 3c). As HP1 also binds to lamina B receptor, which is a nuclear envelope protein bound to the lamina,[43] we speculate that HP1 serves as a lamina buttress to support free movement of flexible chromatin in assembling transcription factories. Using a blocking peptide to disrupt function of HP1, we showed it may be possible to alter the expression of tumor-suppressor genes and simultaneously disassemble the formation of oncogenic regulatory amplicons in cancer cells. As such, our new approach provides a broad and effective therapeutic choice against ERα-positive breast cancers.

It has been shown that DERE amplification correlates to adverse survival of ERα-positive breast cancer patients.[7] To genetically investigate the significance of DEREs in breast cancers, we used CRISPR/Cas9 to precisely delete a DERE region. Recent studies reported that the CRISPR/Cas9 system is a powerful tool for gene-specific targeting in cancer.[26,45–47] In human papillomavirus-related cervical cancers, CRISPR/Cas9 targeting on transcripts of human papillomavirus oncogenes, E6 and E7, and the promoter of human papillomavirus 16 E6/E7 led to accumulation of p53 and p21 proteins for reduced proliferation of cancer cells.[46] Another example is the delivery of CRISPR/Cas9 cassette targeting to tumor-promoting genes leading to attenuation of cancer development in a mouse model.[47] We demonstrated that CRISPR/Cas9 may also be used to precisely delete a regulatory amplicon that controls the expression of multiple JAK/STAT-related genes. This new amplicon-editing approach could be an additional strategy to slow the spread of luminal breast cancer in patients at high risk of developing endocrine resistance.

MATERIALS AND METHODS

Cell culture, inhibitor treatment and neutralization assay
Human breast cancer cell lines (600MPE, BT474, HCC1419, HCC1428, HCC1500, LY2, MCF-7, MDA-MB-175 and SUM52PE) were obtained from the American Type Culture Collection (Manassas, VA, USA). Forty-eight hours before estrogen treatment (17β-estradiol or E2, 70 nM), cells were cultured in regular medium within 5% charcoal dextran-stripped fetal bovine serum for hormone deprivation. In the neutralization assay, hormone-deprived cells were treated with control or HP1-blocking peptide (GeneTex Inc., Irvine, CA, USA) for 2 h in advance and then stimulated with dimethylsulfoxide or E2 for indicated time periods. For epigenetic studies, cells were treated with 1 μM 5-aza-2′-deoxycytidine for 4 days in hormone-deprived conditions. During the final 24 h of hormone deprivation, cells were treated with 1 μM trichostatin A followed by treatment with dimethylsulfoxide or E2 for 4 h. All chemicals were purchased from Sigma Aldrich.

Bioinformatic analyses of 3C-seq, ChIP-seq and methylation data sets
Identification of DERE-mediated chromatin looping events from 3C-seq was conducted as previously described.[7] In brief, integration of ERα ChIP-seq and 3C-seq data sets, an DERE-interacting locus was defined based on the following criterion in which at least one DERE is located within 10 kb of an interactive site. Furthermore, if a DERE is located between 10-kb upstream to transcription start site and terminate site of a gene, this gene is considered to be DERE-targeted locus. A total of 92 loci associated with 20q13 DERE sites were found. Poisson distribution for defining significant binding events in ChIP-seq data and methylation reads from methylation profiling were conducted as previously described.[5,21,22] Methylation reads on each bin divided by the 200-bp bin size were calculated to plot methylation intensity maps of 20q13 DERE sites and the associated flanking regions (−2.5 to +2.5 kb) in nine ERα-positive breast cancer cell lines.

Interphase 3D-FISH and immunofluorescence staining coupled with interphase 3D-FISH (immuno-FISH)
The probes interrogating the 20q13 DERE region and ZIM2 locus were prepared from BACs (Invitrogen). For 3D-FISH, probe preparation using Alexa Fluor 488-dUTP (Molecular Probes) for DERE and Alexa Fluor 568-dUTP for ZIM2 and sample hybridization were conducted as previously described.[7] For immuno-FISH, fixed cells were hybridized to anti-HP1 antibody (Santa Cruz Biotechnology) first, following Alexa Fluor 568-conjugated second antibody. 3D-FISH was then preceded. Images were acquired on an Ultima confocal device (Prairie Technologies, Billerica, MA, USA) with a Nikon Eclipse FN-1 upright microscope (Melville, NY, USA; 60X/1.4NA oil immersion objective) and Prairie View software (version 4.3, Billerica, MA, USA). Image J software (imagej.nih.gov/ij/) was applied for image analyses, including qualification and quantification of DERE clustering and colocalization of DERE-HP1 and DERE-ZIM2. A total of 50 nuclei were scored.

Reverse transcription (RT) and 3C-qPCR
RT–qPCR analysis of 1 μg total RNA and 3C-qPCR analysis of BamHI-digested chromatin with diluted ligation was performed using the StepOne Plus PCR System apparatus (Invitrogen) as previously described.[5,7] See Supplementary Table S1 for the primer information.

Integrated looping-ChIP (3C-ChIP) and ChIP-qPCR
Cells fixed with 1% formaldehyde were subjected to ChIP-qPCR as previously described.[7] ChIP antibodies including HP1 (pAB-071-050), RNA polymerase II

Figure 6. Deletion of DEREs using CRISPR/Cas9 system reduces cancer cell growth and proliferation signaling associated with better survival outcome. (a) Illustration of targeted DERE region subjected to CRISPR/Cas9 genomic-editing system. A CRISPR/Cas9 cassette including a donor plasmid harboring drug-selection marker-puromycin (PuroR) and a pCRISPR plasmid containing Cas9 and two specific sgRNAs precisely targeting to the 1-kb DERE region of interest or one scramble sgRNA was applied. Two primer sets for PCR analyses were used to confirm the deletion of DERE region. (b) PCR analysis of the examined DERE region in MCF-7 cells and DERE/del mutants. A gel picture illustrated PCR results of the examined DERE region in MCF-7 cells with transfection of a control CRISPR/Cas9 cassette (Ctrl) and two identified DERE-deleted mutants (DERE/del #1 and #2). The DERE/del #2 was chosen for cell proliferation assay in c and expression analysis of DERE-targeted genes in (d). (c) Cell proliferation analysis of MCF-7 (Ctrl) and DERE/del #2 cells. Growth curves of cells were monitored and plotted for continuous 72 h using IncuCyte ZOOM live cell image device. (d) Twelve representative examples of DERE/del-directed transcription control. RT–qPCR analysis of DERE-targeted genes was assayed in MCF-7 (Ctrl) and DERE/del cells. Mean ± s.d. (n = 3). *P < 0.05; **P < 0.01; ***P < 0.001 (Student's t-test), compared with 'Ctrl' cells. See also Supplementary Figure S8 for expression results of additional 21 loci. (e) Ingenuity pathway analysis (IPA) of DERE/del-altered loci was used to determine JAK/STAT signaling associated with DERE deletion. Green ovals: DERE/del-repressed genes; red ovals: DERE/del-activated genes; blue ovals: gene associated with anti-proliferation signaling. (f and g) Correlation analysis between DERE/del-altered transcription and overall survival of ERα-positive breast cancer patients. Kaplan–Meier analysis was conducted on two expression data sets of non-relapse ERα-positive breast tumors, which include 129 patients in (f) and 227 patients with 5-year tamoxifen treatment in (g),[37,38] respectively. Mantel–Cox test was used to determine statistical significance.

(RNA Pol II; AC-055-100), H3K4me3 (pAB-003-050), H3K9ac (C15410004), H3K9me3 (C15310013), H3K27ac (C15410174) and H3K27me3 (CS-069-100) were from Diagenode (Denville, NJ, USA) and ERα (sc-8005X) was purchased from Santa Cruz Biotechnology. For 3C-ChIP-qPCR analyses, *Bam*HI-digested 3C samples were dilutely ligated and then subjected to ChIP-qPCR analysis. See Supplementary Table S1 for the primer information.

Establishment of DERE/del mutants using CRISPR/Cas9 genomic-editing system

The target-specific CRISPR/Cas9 cassette including two plasmids—a donor plasmid harboring puromycin selection marker and a pCRISPR plasmid with Cas9 and two specific sgRNAs precisely targeting to the interested 1-kb 20q13 DERE region is constructed and validated by GeneCopoeia (Rockville, MD, USA). For demonstrating the specificity of the target-specific CRISPR constructs, a control pCRISPR plasmid harboring Cas9 and one scramble sgRNA is also applied. MCF-7 cells were transfected with either target-specific or control CRISPR cassette using X-tremeGene HP Transfection Reagent (Roche Applied Science, Indianapolis, IN, USA). Validation of DERE/del mutants selected by puromycin was conducted using PCR analysis coupled with 0.8% agarose electrophoresis. The applied primer sets are as follows: primer #1, 5′-CCTGGCTCCAAAGTATACTC-3′ and 5′-ACACTATGATGAGCAGAGGG-3′; Primer #2, 5′-ACCCGTCATGAGCAACTCC-3′ and 5′-GGCCAGGCTGTTCTCAAAC-3′.

siRNA transfections

MCF-7 cells (10^6 cells) were seeded in a 10-cm dish and transfected the next day with siRNA against HP1 (SMARTpool siRNA, Dharmacon, Lafayette, CO, USA) using the Fugene HD transfection reagent (Roche, Indianapolis, IN, USA) according to the manufacturer's protocol. Culture media were switched to contain 5% charcoal dextran serum. After 48 h, the cells were treated with E2 (70 nM) in 1 h for ChIP-qPCR and 3C-ChIP-qPCR analyses or different time periods (0, 0.5, 1, 4, 24 h) for RT–qPCR analysis. Scrambled oligonucleotide was applied as a negative control.

Cell proliferation assay

Control or HP1-blocking peptide-treated cells and DERE/del #2 cells (10^4 cells per well) seeded on a 96-well plate were monitored in continuous 3 days using the IncuCyte ZOOM live cell image device (Essen Bioscience, Ann Arbor, MI, USA) for cell proliferation. Cells with HP1 siRNA treatment and DERE/del #3 were subjected to Vybrant MTT Cell Proliferation Assay (Invitrogen) following the manufacturer's protocol and iMark Microplate Reader (Bio-Rad, Hercules, CA, USA) was used to determine absorbance.

Statistical analyses

qPCR results were presented as the mean ± s.d. of *n* independent measurements. GraphPad Prism 6 (La Jolla, CA, USA) was used for statistical comparisons between two groups made by Student's *t*-test, survival analyses made by Mantel–Cox test and plotting Kaplan–Meier survival curves.

CONFLICT OF INTEREST

The authors declare no conflict of interest.

REFERENCES

1 Brisken C, O'Malley B. Hormone action in the mammary gland. *Cold Spring Harb Persepct Biol* 2010; **2**: a003178.

2 Thomas C, Gustafsson JÅ. The different roles of ER subtypes in cancer biology and therapy. *Nat Rev Cancer* 2011; **11**: 597–608.

3 Cicatiello L, Mutarelli M, Grober OM, Paris O, Ferraro L, Ravo M *et al*. Estrogen receptor alpha controls a gene network in luminal-like breast cancer cells comprising multiple transcription factors and microRNAs. *Am J Pathol* 2010; **176**: 2113–2130.

4 Carroll JS, Meyer CA, Song J, Li W, Geistlinger TR, Eeckhoute J *et al*. Genome-wide analysis of estrogen receptor binding sites. *Nat Genet* 2006; **38**: 1289–1297.

5 Hsu PY, Hsu HK, Singer GA, Yan PS, Rodriguez BA, Liu JC *et al*. Estrogen-mediated epigenetic repression of large chromosomal regions through DNA looping. *Genome Res* 2010; **20**: 733–744.

6 Fullwood MJ, Liu MH, Pan YF, Liu J, Xu H, Mohamed YB *et al*. An oestrogen-receptor-alpha-bound human chromatin interactions. *Nature* 2009; **462**: 58–64.

7 Hsu PY, Hsu HK, Lan X, Juan L, Yan PS, Labanowska J *et al*. Amplification of distant response elements deregulates target genes associated with tamoxifen resistance in breast cancer. *Cancer Cell* 2013; **24**: 197–212.

8 Sutherland H, Bickmore WA. Transcription factories: gene expression in unions? *Nat Rev Genet* 2009; **10**: 457–466.

9 Michell JA, Fraser P. Transcription factories are nuclear subcompartments that remain in the absence of transcription. *Genes Dev* 2008; **22**: 20–25.

10 Deng B, Melnik S, Cook PR. Transcription factories, chromatin loops, and the dys-regulation of gene expression in malignancy. *Semin Cancer Biol* 2013; **23**: 65–71.

11 Papantonis A, Cook PR. Transcription factories: genome organization and gene regulation. *Chem Rev* 2013; **113**: 8683–8705.

12 Ulbricht T, Alzrigat M, Horch A, Reuter N, von Mikecz A, Steimle V *et al*. PML promotes MHC class II gene expression by stabilizing the class II transactivator. *J Cell Biol* 2012; **199**: 49–63.

13 Sleeman JE, Trinkle-Mulcahy L. Nuclear bodies: new insights into assembly/dynamics and disease relevance. *Curr Opin Cell Biol* 2014; **28**: 76–83.

14 Papantonis A, Kohro T, Baboo S, Larkin JD, Deng B *et al*. TNFα signals through specialized factories where responsive coding and miRNA genes are transcribed. *EMBO J* 2012; **31**: 4404–4414.

15 Cai S, Lee CC, Kohwi-Shigematsu T. SATB1 packages densely looped, transcriptionally active chromatin for coordinated expression of cytokine genes. *Nat Genet* 2006; **38**: 278–288.

16 Gaszner M, Felsenfeld G. Insulators: exploiting transcriptional and epigenetic mechanisms. *Nat Rev Genet* 2006; **7**: 703–713.

17 Beisel C, Paro R. Silencing chromatin: comparing modes and mechanisms. *Nat Rev Genet* 2011; **12**: 123–135.

18 Harmston N, Lenhard B. Chromatin and epigenetic features of long-range gene regulation. *Nucleic Acids Res* 2013; **41**: 7185–7199.

19 Ong CT, Corces VG. Enhancers: emerging roles in cell fate specification. *EMBO Rep* 2012; **13**: 423–430.

20 Zhang CZ, Leibowitz ML, Pellman D. Chromothripsis and beyond: rapid genome evolution from complex chromosomal rearrangements. *Genes Dev* 2013; **27**: 2513–2530.

21 Joseph R, Orlov YL, Huss M, Sun W, Kong SL, Ukil L *et al*. Integrative model of genomic factors for determining binding site selection by estrogen receptor-α. *Mol Syst Biol* 2010; **6**: 456–468.

22 Gu F, Doderer MS, Huang YW, Roa JC, Goodfellow PJ, Kizer EL *et al*. CMS: a web-based system for visualization and analysis of genome-wide methylation data of human cancers. *PLoS One* 2013; **8**: e60980.

23 Osborne CS, Chakalova L, Mitchell JA, Horton A, Wood AL, Bolland DJ *et al*. Myc dynamically and preferentially relocates to a transcription factory occupied by Igh. *PLoS Biol* 2007; **5**: e192.

24 Yamada T, Fukuda R, Himeno M, Sugimoto K. Functional domain structure of human heterochromatin protein HP1 Has: involvement of internal DNA-building DNA-binding and C-terminal self-association domains in the formation of discrete dots in interphase nuclei. *J Biochem* 1999; **125**: 832–837.

25 Kim J, Bergmann A, Lucas S, Stone R, Stubbs L. Lineage-specific imprinting and evolution of the zinc-finger gene ZIM2. *Genomics* 2004; **84**: 47–58.

26 Hsu PD, Lander ES, Zhang F. Development and applications of CRISPR-Cas9 for genome engineering. *Cell* 2014; **157**: 1262–1278.

27 Zhang X, Zhang L, Yang H, Huang X, Otu H, Libermann TA *et al*. c-Fos as a proapoptotic agent in TRAIL-induced apoptosis in prostate cancer cells. *Cancer Res* 2007; **67**: 9425–9434.

28 Kalra N, Kumar V. c-Fos is a mediator of the c-myc-induced apoptotic signaling in serum-deprived hepatoma cells via the p38 mitogen-activated protein kinase pathway. *J Biol Chem* 2004; **279**: 25313–25319.

29 Kwak HI, Gustafson T, Metz RP, Laffin B, Schedin P, Porter WW. Inhibition of breast cancer growth and invasion by single-minded 2 s. *Carcinogenesis* 2007; **28**: 259–266.

30 Feng X, Wang Y, Ma Z, Yang R, Liang S, Zhang M *et al*. MicroRNA-645, up-regulated in human adenocarcinoma of gastric esophageal junction, inhibits apoptosis by targeting suppressor IFIT2. *BMC Cancer* 2014; **14**: 633.

31 Sciacovelli M, Guzzo G, Morello V, Frezza C, Zheng L, Nannini N et al. The mito-chondrial chaperone TRAP1 promotes neoplastic growth by inhibiting succinate dehydrogenase. Cell Metab 2013; 17: 988–999.

32 Protty MB, Watkins NA, Colombo D, Thomas SG, Heath VL, Herbert JM et al. Identification of Tspan9 as a novel platelet tetraspanin and the collagen receptor GPVI as a component of tetraspanin microdomains. Biochem J 2009; 417: 391–400.

33 Ma D, Hovey RL, Zhang Z, Fye S, Huettner PC, Borecki IB et al. Genetic variation in EGFR and ERBB4 increase susceptibility to cervical cancer. Gynecol Oncol 2013; 131: 445–450.

34 Springuel L, Hornakova T, Losdyck E, Lambert F, Leroy E, Constantinescu SN et al. Cooperation JAK1 and JAK3 mutants increase resistance to JAK inhibitors. Blood 2014; 24: 3924–3931.

35 Qi J, Li N, Fan K, Yin P, Zhao C, Li Z et al. β1,6 GlcNAc branches-modified PTPRT attenuates its activity and promotes cell migration by STAT3 pathway. PLoS One 2014; 9: e98052.

36 Hoffman B, Liebermann DA. Apoptotic signaling by c-MYC. Oncogene 2008; 27: 6462–6472.

37 Wang Y, Klijn JG, Zhang Y, Sieuwerts AM, Look MP, Yang F et al. Gene-expression profiles to predict distant metastasis of lymph-node-negative primary breast cancer. Lancet 2005; 365: 671–679.

38 Symmans WF, Hatzis C, Sotiriou C, Andre F, Peintinger F, Regitnig P et al. Genomic index of sensitivity to endocrine therapy for breast cancer. J Clin Oncol 2010; 28: 4111–4119.

39 Chin K, DeVries S, Fridlyand J, Spellman PT, Roydasgupta R, Kuo WL et al. Genomic and transcriptional aberrations linked to breast cancer pathophysiologies. Cancer Cell 2006; 10: 529–541.

40 Ginestier C, Cervera N, Finetti P, Esteyries S, Esterni B, Adélaïde J et al. Prognosis and gene expression profiling of 20q13-amplified breast cancers. Clin Cancer Res 2006; 12: 4533–4544.

41 Santarius T, Shipley J, Brewer D, Stratton MR, Cooper CS. A census of amplified and overexpressed human cancer genes. Nat Rev Cancer 2010; 10: 59–64.

42 Misteli T. Higher-order genome organization in human disease. Cold Spring Harb Perspect Biol 2010; 2: a000794.

43 Fahrner JA, Baylin SB. Heterochromatin: stable and unstable invasions at home and abroad. Genes Dev 2003; 17: 1805–1812.

44 Sharma RP, Gavin DP, Chase KA. Heterochromatin as an incubator for pathology and treatment non-response: implication for neuropsychiatric illness. Pharmaco-genomics J 2012; 12: 361–367.

45 Cong L, Ran FA, Cox D, Lin S, Barretto R, Habib N et al. Multiplex genome engi-neering using CRISPR/Cas systems. Science 2013; 339: 819–823.

46 Zhen S, Hua L, Takahashi Y, Narita S, Liu YH, Li Y. In vitro and in vivo growth suppression of human papillomavirus 16-positive cervical cancer cells by CRISPR/Cas9. Biochem Biophys Res Commun 2014; 450: 1422–1426.

47 Xue W, Chen S, Yin H, Tammela T, Papagiannakopoulos T, Joshi NS et al. CRISPR-mediated direct mutation of cancer genes in the mouse liver. Nature 2014; 514: 380–384.

Supplementary Information accompanies this paper on the Oncogene website (http://www.nature.com/onc)